Available online at www.sciencedirect.com
ScienceDirect
Journal of the European Ceramic Society 31 (2011) 217–224
www.elsevier.com/locate/jeurceramsoc

Mechanical properties of low temperature synthesized dense and fine-grained Cr_2AlC ceramics

S.B. Li [a,b,*], W.B. Yu [a], H.X. Zhai [a], G.M. Song [b], W.G. Sloof [b], S. van der Zwaag [c]

[a] *Institute of Materials Science and Engineering, School of Mechanical and Electronic Control Engineering, Beijing Jiaotong University, Beijing 100044, China*
[b] *Department of Materials Science and Engineering, Delft University of Technology, Mekelweg 2, 2628 CD Delft, The Netherlands*
[c] *Novel Aerospace Materials Group, Faculty of Aerospace Engineering, Delft University of Technology, Kluyverweg 1, 2629 HS Delft, The Netherlands*

Received 20 May 2010; received in revised form 6 August 2010; accepted 10 August 2010
Available online 17 September 2010

Abstract

Mechanically activated hot-pressing technology was used to synthesize a fine-crystalline Cr_2AlC ceramic at relatively low temperatures. A mixture of Cr, Al and C powders with a molar ratio of 2:1.2:1 was mechanically alloyed for 3 h, and then subjected to hot pressing at 30 MPa and different temperatures for 1 h in Ar atmosphere. The results show that a dense Cr_2AlC ceramic with a grain size of about 2 μm can be synthesized at a relatively low temperature of 1100 °C. The synthesized fine-grained Cr_2AlC has a high density of 99%, which is higher than the 95% density for the coarse-grained Cr_2AlC (grain size of about 35 μm) as synthesized by hot pressing unmilled Cr, Al and C. The flexural strength, fracture toughness and Vickers hardness of the fine-grained Cr_2AlC were determined and compared with the values for the coarse-grained Cr_2AlC.

Keywords: Cr_2AlC; Carbides; Mechanically activated hot pressing; Microstructure; Mechanical properties

1. Introduction

MAX phase ceramics (where M denotes an early transition metal, A is an element mostly in IIIA or IVA group, and X is either C or N) exhibit many unusual combinations of attractive properties such as a high electrical conductivity, a low oxidation rate, resistance against corrosion, and high strength at high temperature as well as good machinability.[1,2] Moreover, these materials show autonomous crack healing at high temperatures in an oxidizing environment.[3] Out of the total MAX phase family, the systems Ti_3SiC_2, Ti_3AlC_2 and Ti_2AlC have been studied extensively because of their attractive properties and relative ease of fabrication. Recently it has been shown that Cr_2AlC has an even better oxidation and corrosion resistance than Ti_3SiC_2 and Ti_3AlC_2 at high temperatures.[4–6] So, Cr_2AlC is expected to be a more promising candidate for high temperature applications. In addition, the thermal expansion of Cr_2AlC is 12–13 × 10^{-6}/K, which is close to that of the superalloys.[7,8] Hence Cr_2AlC has potential applications in the field of ceramics/metals joining and protective coatings on the superalloys. The possibility of depositing large area Cr_2AlC coatings on steel substrates has already been demonstrated.[9]

There are several methods used to produce Cr_2AlC bulk ceramics. For example, Manoun et al.[10] synthesized Cr_2AlC bulk ceramic by hot isostatic pressing (HIP) of a mixture of 2Cr/Al/C elemental powders at 1200 °C under 100 MPa for 12 h. Lee and Nguyen[6] obtained Cr_2AlC bulk ceramic by hot pressing powders of $CrC_{0.5}$ and Al at 1300 °C under 25 MPa for 1 h. No information was provided on the presence of other phases. Lin et al.[11] made Cr_2AlC bulk ceramic with 95% density and containing Al–Cr phase as an impurity by hot pressing a mixture of 2Cr/1.05Al/C at 1400 °C under 30 MPa for 1 h. Tian et al.[12] fabricated Cr_2AlC bulk ceramic with Cr_7C_3 as the impurity by hot pressing a mixture of 2Cr/1.1Al/C at 1400 °C under 30 MPa for 1 h. They[13] also fabricated the ceramic by pulse discharge sintering (PDS) the same mixture at 1250 °C under 50 MPa for 30 min. Impurities of Al_2O_3 and Cr_7C_3 were detected in the matrix.

Generally, it is difficult to produce a pure Cr_2AlC ceramic from a mixture of Cr, Al and C powders, due to the formation of intermediate compounds, such as Al_4C_3, Cr_7C_3 and Cr–Al

* Corresponding author at: Institute of Materials Science and Engineering, School of Mechanical and Electronic Control Engineering, Beijing Jiaotong University, Beijing 100044, China. Tel.: +86 10 51685554; fax: +86 10 51685554.
E-mail address: shbli1@bjtu.edu.cn (S.B. Li).

0955-2219/$ – see front matter © 2010 Elsevier Ltd. All rights reserved.
doi:10.1016/j.jeurceramsoc.2010.08.014

phases.[4–7,10–13] For high temperature structural applications a high density is prerequisite. The densities of Cr_2AlC ceramics synthesized by HP of a mixture of Cr, Al and C powders are about 95–97%.[11,12] To produce Cr_2AlC ceramics with a higher density, mechanically activated sintering (MAS) technology has been adopted. Then, the ceramic can be fabricated at relatively low temperatures as has been demonstrated for Ti_3SiC_2,[14] Ti_3AlC_2[15] and Ti_2SnC.[16] The MAS process makes use of mechanically alloyed powders with a superfine structure that are subsequently sintered. These pre-milled powders exhibit a high reactivity due to their high lattice defect density, large grain boundary area and large internal strains, which lead to a relatively low synthesis temperature. In addition, the MAS technology can be used to make fine powders and also obtain dense ceramics with nano-sized microstructure from low cost starting powders.

In this paper, the production of Cr_2AlC ceramic by mechanically activated sintering is described and the microstructure and mechanical properties of the produced dense materials are presented.

2. Experimental procedures

Powders of Cr (particle size <75 μm, >99 wt.% purity, Beijing Reagent Company, Beijing, China), Al (particle size <75 μm, 99.5 wt.% purity, Beijing Reagent Company) and C (graphite, particle size <45 um, 99.5 wt.% purity, General Research Institute for Nonferrous Metals, Beijing, China) were used as the starting materials. The designed molar ratio of Cr, Al and C powders was Cr:Al:C = 2:1.2:1 to make Cr_2AlC samples. Extra Al was used to compensate for the loss of Al during the sintering process.

Mechanical alloying was performed in a QM-1SP4 planetary ball mill (Nanjing, China) using stainless steel containers and balls. The weight ratio of ball to powder was 20:1. The containers were evacuated to a pressure of 1×10^{-2} Pa. The rotation speed of the containers was set to 500 rpm. To avoid excessive heating during the milling process, the container surface was cooled in water for 10 min during milling at intervals of 0.5 h. A small amount of the milled powders was taken out of the containers after milling at various times for X-ray diffraction (XRD) analysis with a D/Max 2200 PC diffractometer (Tokyo, Japan) using Cu Kα radiation.

The mechanically activated powders were hot pressed at different temperatures for 1 h under 30 MPa in an Ar atmosphere. The heating rate was 30 °C/min. For comparison, unmilled Cr, Al and C powders were only mixed for 10 h and then hot pressed at 1450 °C under 30 MPa for 1 h in Ar.

The phase composition and the microstructure of the samples were identified with XRD and scanning electron microscopy (SEM) using a JEOL JSM 6500F field emission gun scanning electron microscope (Tokyo, Japan), which was equipped with energy-dispersive spectroscopy (EDS). Specimen for transmission electron microscopy (TEM) observation using a JEOL JEM 4000EX (Tokyo, Japan) was prepared by slicing, grinding and ion milling. The samples were polished using a JEOL SM09010 cross-section ion polisher (Tokyo, Japan) for SEM observation. The density of the samples was measured by the water immersion technique. The average grain size was obtained from the average linear intercept length comprising at least 100 grains in SEM micrographs taken of the fracture surfaces of the synthesized samples, multiplied with a statistical factor of 1.56.[17]

The Vickers hardness was determined with a Zwick/Z2.5 hardness tester (Ulm, Germany) in a load range of 1–50 kg and at a constant contact time of 15 s. The flexural strength of 3 mm × 4 mm × 36 mm specimens was measured by a three-point bending test using a Deben Microtester (Woolpit, UK). The span size and crosshead speed were 30 mm and 0.5 mm/min, respectively. The fracture toughness was measured using the single edge notched beam method. 2 mm × 4 mm × 36 mm specimens with a notch of about 2 mm in depth and 0.2 mm in width were used. Span size was 30 mm, and crosshead speed was 0.05 mm/min.

3. Results and discussion

3.1. Microstructure

The XRD patterns of the mixture of Cr, Al and C powders with a molar ratio of Cr:Al:C = 2:1.2:1 (denoted as 2Cr/1.2Al/C) before and after milling for 1–3 h are shown in Fig. 1. The mixture of powders before milling consists of bcc Cr, fcc Al and graphite C (see Fig. 1(a)). After milling this mixture for only 1 h, the peak in the diffractogram belonging to C (graphite) has completely disappeared, suggesting that either graphite is transformed to an amorphous structure or has already diffused into the surrounding metallic grains (see Fig. 1(b)). This observation is in agreement with those of the previous studies where

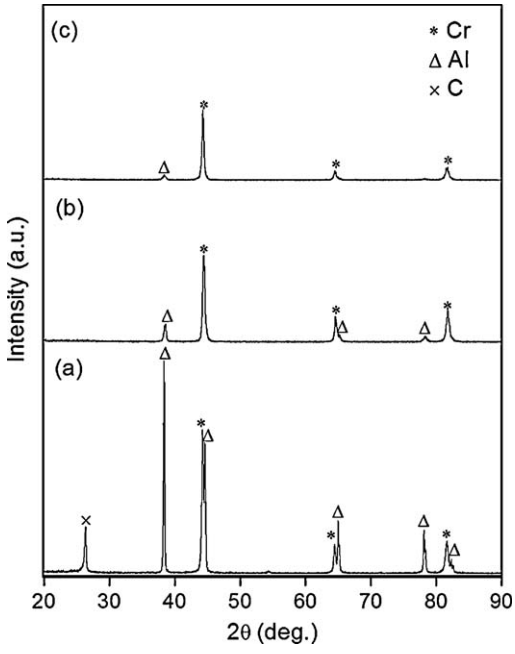

Fig. 1. XRD patterns of 2Cr/1.2Al/C mixture after milling for (a) 0 h, (b) 1 h and (c) 3 h. ICDD card numbers for Cr, Al and graphite are 01-085-1336, 01-089-2837 and 00-001-0640, respectively.

Ti/Si/C, Ti/Al/C and Ti/Sn/C powders were milled for only 1 h.[14–16] Yang et al.[18] found amorphous C after ball milling of Si and graphite powders for 6 h using high-resolution electron microscopy (HREM). Ghosh et al.[19] also identified the existence of the amorphous C film after ball milling of Ni and graphite powders for 3 h using HREM.

The peak intensities of both fcc Al and bcc Cr decreased as a function of milling time. In conjunction with this decrease of peak intensities, broadening of the diffraction lines occurred; see Fig. 1(b)and (c). The observed changes of the diffraction line profiles are associated with a reduction of the coherent domain size and an increase of microstrains due to the development of lattice defects upon milling.[20] Assuming that the broadening of the diffraction line is predominantly determined by the crystallite domain size, then the Al and Cr crystallite domain size according to the Scherrer formula[21] decrease to 20–30 nm after 1–3 h of milling.

No Cr–Al compound or carbide phase was identified with XRD after ball milling for 3 h (see Fig. 1(c)), indicating that no detectable reaction between the elements occurred during the milling process. In general, a long-time ball milling can introduce Fe from the steel balls and container as an impurity into the final product. However, neither diffraction lines of bcc Fe nor Fe was detected with X-ray microanalysis of the final product. The main reason for the absence of Fe in the milled powders should be attributed to the short milling time of 3 h. The other may be attributable to that the soft Al coats the surfaces of the grinding balls and the inner walls of the container during the early milling stage, preventing the contamination of the milled powders. It has been demonstrated that one way of minimizing the contamination during milling is to shorten the milling time or use a milled material to form a thin adherent coating on the surface of the grinding medium and also on the internal surface of the container.[22]

XRD patterns of the mechanically alloyed (MA) 2Cr/1.2Al/C powders after hot pressing at various temperatures in the range of 850–1100 °C are shown in Fig. 2. After hot pressing at 850 °C, the main phase is Cr_2AlC with small amounts of $AlCr_2$, $Cr_{23}C_6$ and Cr (see Fig. 2(a)). The sample synthesized at 1000 °C consists mainly of the Cr_2AlC phase plus minor amounts of $AlCr_2$ (see Fig. 2(b)). Increasing the hot pressing temperature to 1100 °C, only Cr_2AlC phase was detected, indicating that an almost pure Cr_2AlC ceramic was obtained (see Fig. 2(c)). In contrast with sintering of a conventional mixture of coarser Cr, Al and C powders where Cr_2AlC formation started to form at a sintering temperature of 1050 °C,[11] the mechanically alloyed powders formed Cr_2AlC already at a sintering temperature of 850 °C.

Compared with the sintering temperature of 1400 °C reported for achieving Cr_2AlC ceramics by hot pressing the conventional mixture of Cr, Al and C powders,[4,5,11,12] the present synthesis temperature is decreased by about 300 °C. This can be attributed to the mechanically alloying of the starting powders which possess enhanced reactivity because of their nano-structure, high defect densities and large internal strains. During mechanical alloying, the powders were subjected to repeatedly welding and fracture resulting not only in a reduction of the particle size but also in a high defect density and large internal strains. Consequently, the diffusion processes are accelerated due to this particle refinement which increases the area of contact between the reactant powder particles and reduces the diffusion distances. Hence, the reaction temperatures will be significantly lower as compared with hot pressing of unmilled powders.[14–16,21]

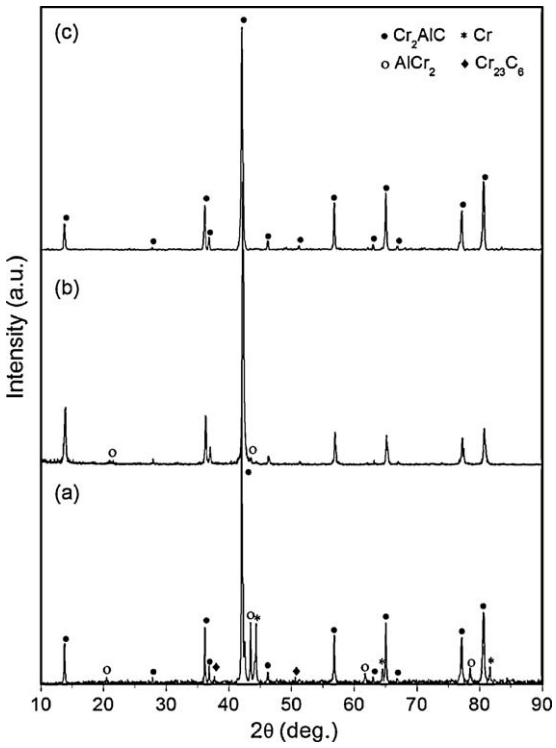

Fig. 2. XRD patterns of mechanically alloyed 2Cr/1.2Al/C powders after hot pressing at (a) 850 °C, (b)1000 °C, and (c)1100 °C under 30 MPa for 1 h in Ar. ICDD card numbers for Cr_2AlC, Cr, $AlCr_2$ and $Cr_{23}C_6$ are 01-089-2275, 01-085-1336, 03-065-6360 and 01-085-1281, respectively.

Therefore Cr_2AlC might even form at temperatures lower than 850 °C. So further work was performed to study the reactions in the MA 2Cr/1.2Al/C powders at 600 and 700 °C.

The phase compositions after hot pressing the MA 2Cr/1.2Al/C powders at 600 and 700 °C for 1 h, respectively, are shown in Fig. 3. Cr_2AlC, $AlCr_2$ and unreacted Cr are detected. It should be noted that Cr_2AlC and $AlCr_2$ phases start to form at 600 °C (see Fig. 3(a)). After hot pressing at 700 °C, the diffraction lines belonging to Cr_2AlC become strong, due to the increase amount of Cr_2AlC phase and the crystallite domain growth (see Fig. 3(b)). Peak corresponding to C is not found in the XRD patterns, probably due to the formation of amorphous C-phase induced by mechanical alloying. Further, no Cr–C carbides are detected at temperature below 700 °C, probably due to their low content below the detection limit of the XRD or the reaction of C and Cr starting above 700 °C.

Using the results presented above, the reaction sequence in the MA 2Cr/1.2Al/C system might be described as follows: firstly, Al reacts with Cr to form $AlCr_2$. The formation of $AlCr_2$ at about 600 °C, lower than the melting point of Al (660 °C), has an obvious advantage of preventing the loss of Al at high temperature. Secondly, the formed $AlCr_2$ reacts with amorphous C induced by MA to form Cr_2AlC at about 600 °C. This reac-

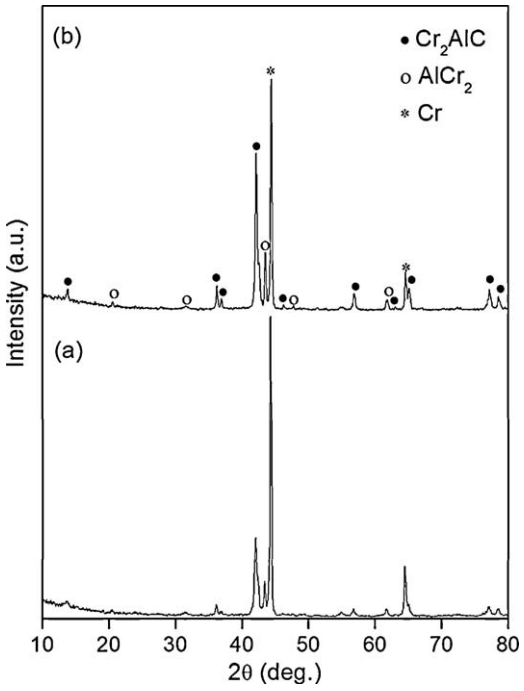

Fig. 3. XRD patterns of mechanically alloyed 2Cr/1.2Al/C powders after hot pressing at (a) 600 °C and (b) 700 °C under 30 MPa for 1 h in Ar. ICDD card numbers for Cr_2AlC, Cr and $AlCr_2$ are 01-089-2275, 01-085-1336, and 03-065-6360, respectively.

tion also explains the reason why $AlCr_2$ appeared at 1000 °C (Fig. 2(b)) but disappeared at 1100 °C (Fig. 2(c)). Thirdly, unreacted Cr reacts with C, forming a Cr–C compound at above 700 °C, which is $Cr_{23}C_6$ according to the XRD result as shown in Fig. 2(a). With increasing temperature, the intermediate phases of $AlCr_2$ and $Cr_{23}C_6$ are consumed completely and only the single Cr_2AlC phase is left.

However, in the conventional Cr, Al and C reaction system, Al first melts at above 660 °C, and then reacts with Cr to form Cr–Al compounds (i.e. Cr_9Al_{17}, Al_8Cr_5 and $AlCr_2$) at above 670 °C. Cr_2AlC starts to form at 1050 °C via a reaction among Al–Cr compounds, Cr and C or a reaction between $AlCr_2$ and C.[11,23] By comparison, the reactivity of MA 2Cr/1.2Al/C powder is enhanced. The enhanced reactivity was also proved by MA of Ti, Al and C powders. Previous research showed that a reaction between Ti and Al already occurred at a temperature below the melting point of Al.[24–26] But when using conventional Ti, Al and C powders, the reaction between Ti and Al to form a Ti–Al compound occurred at above 720 °C.[27,28]

The measured density of Cr_2AlC made by MAS after sintering at 1100 °C is 5.19 g/cm^3, which is 99% of its theoretical density of 5.24 g/cm^3. This Cr_2AlC material is more dense than that produced by sintering at 1450 °C of a conventional (i.e. not mechanically alloyed) mixture of Cr, Al and C powders, which has a density of only 95%. The lower density of the conventionally produced Cr_2AlC material is probably due to evaporation of low melting point intermetallic phases such as 910 °C for $AlCr_2$ and 1320 °C for Al_8Cr_5 according to the Cr–Al binary phase diagram.[29] At temperatures of 1400–1450 °C applied to synthesize Cr_2AlC from untreated Cr, Al and C powders, significant amounts of liquid intermetallic phases evaporate and leave pores behind. In the present study, there are not much of such liquid phases, and the low synthesis temperature of 1100 °C prevents the evaporation of these phases.

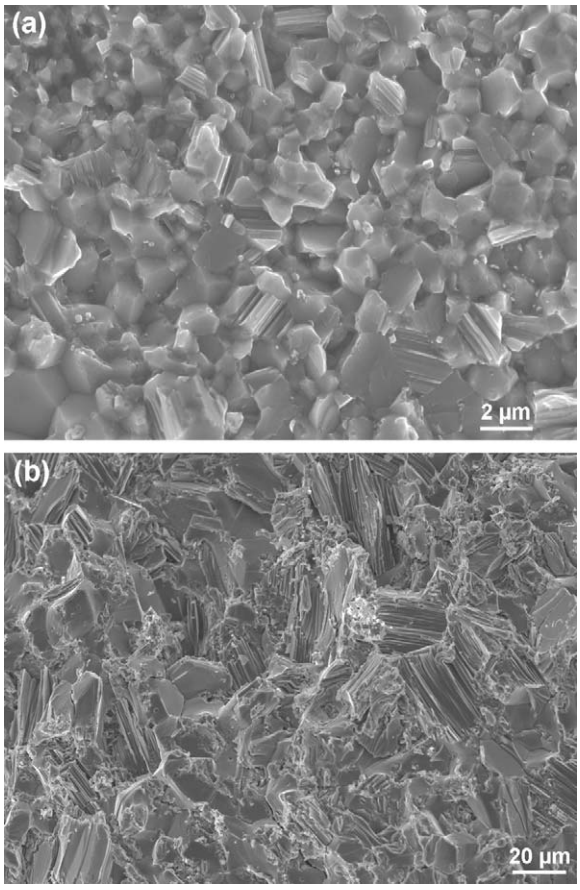

Fig. 4. SEM images of the fracture surfaces of (a) fine-grained Cr_2AlC and (b) coarse-grained Cr_2AlC.

Also as a consequence of the low synthesis temperature of 1100 °C, the Cr_2AlC produced with MAS exhibits a fine-grained microstructure with average grain size of 2 μm, see Fig. 4(a). In comparison, the Cr_2AlC produced with HP of unmilled powders at a temperature of 1450 °C displays a coarse-grained microstructure with an average grain size of 35 μm (see Fig. 4(b)).

A typical backscattered SEM image of an ion polished fine-grained Cr_2AlC sample shows some smaller dark particles distributed in the grains and at the grain boundaries (see Fig. 5(a)). They are probably Al_2O_3 particles based on their EDS signal. A bright-field TEM image and selected-area electron diffraction pattern (SAED) analysis shown in Fig. 5(b) further confirmed the existence of Al_2O_3. Oxygen may be from the original powder or absorbed by the mechanically alloyed powders. During heating, the oxygen reacts with Al to form Al_2O_3.

3.2. Mechanical properties

The measured flexural strength of Cr_2AlC made by MAS is 513 ± 13 MPa, which is significantly higher than that produced

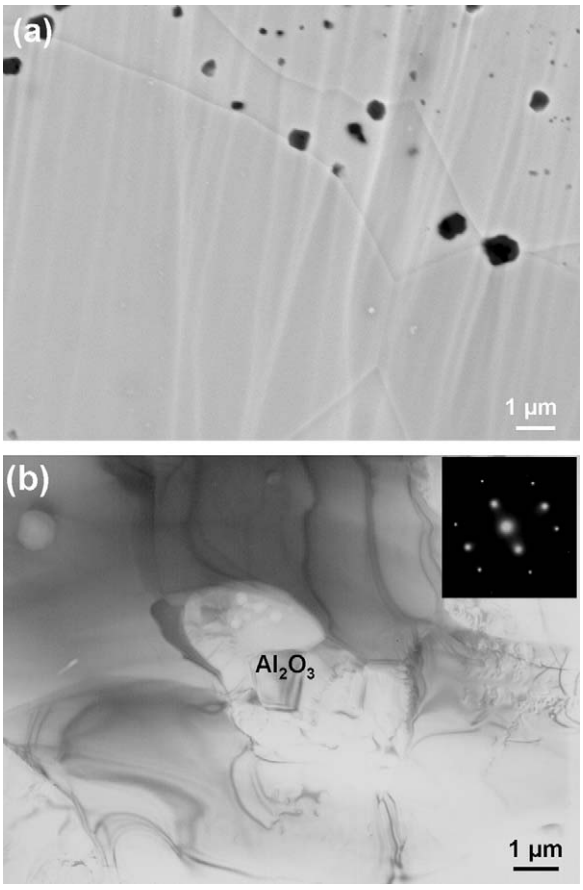

Fig. 5. (a) Backscattered SEM image of polished fine-grained Cr_2AlC. Black particles are Al_2O_3. (b) Bright-field TEM image for fine-grained Cr_2AlC. Inset is the selected-area electron diffraction pattern for Al_2O_3.

by HP from the unmilled powders, viz. 305 ± 10 MPa. This large difference in flexural strength between the two Cr_2AlC materials produced can be explained from the observed differences in microstructure, i.e. grain size and density (see above). The fracture mode of the fine-grained Cr_2AlC ceramic is mainly intergranular (Fig. 4(a)), whereas that of the coarse-grained Cr_2AlC ceramic is mainly transgranular (Fig. 4(b)). The fracture toughness of the fine-grained Cr_2AlC ceramic is

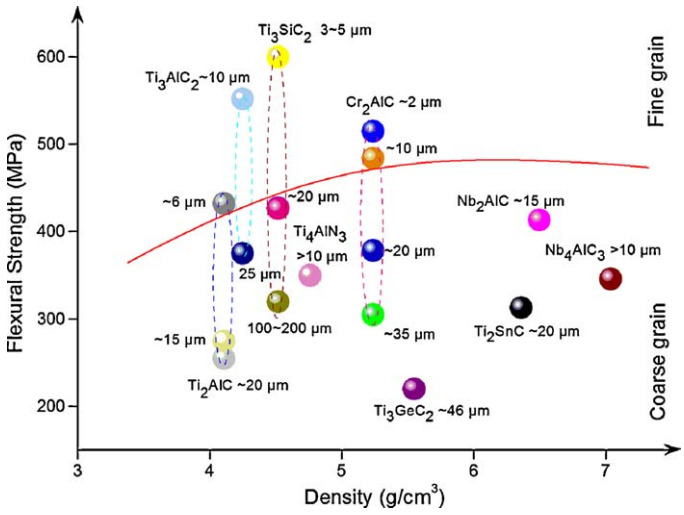

Fig. 6. Map of flexural strength versus density of MAX phase ceramics. The dashed areas reflect the wide range of strength caused by grain size for the same material. The areas above and below the red line represent the flexural strength caused by the fine (≤10 μm) and coarse (>10 μm) grain sizes of the MAX ceramics, respectively.

4.7 ± 0.2 MPa m$^{1/2}$, which is lower than 6.2 MPa m$^{1/2}$ for the coarse material.

For comparison, the typical mechanical properties of Cr_2AlC made by different methods are listed in Table 1. It is clear that the Vickers hardness and flexural strength of Cr_2AlC made by MAS are high.

Compared with other known MAX phase ceramics, the flexural strength of the fine-grained Cr_2AlC is amongst the highest of the "211" phase series (see Fig. 6). Further, the grain size dependence of the flexural strength is also seen for other MAX phase ceramics, i.e. "413" phase series of Ti_4AlN_3 and Nb_4AlC_3, "312" phase series of Ti_3SiC_2, Ti_3GeC_2 and Ti_3AlC_2, "211" of Ti_2AlC, Ti_2SnC, Nb_2AlC and Cr_2AlC (see Fig. 6).[1,12,30–41] Theoretical studies on the electronic structure and bond energy of the MAX materials have shown that the mechanical properties of MAX materials are determined primarily by the M–X layers.[42,43] Cr_2AlC has the highest C–Cr bond energy of all

Table 1
Mechanical properties for Cr_2AlC.

Flexural strength (MPa)	Fracture toughness (MPa m$^{1/2}$)	Vickers hardness (GPa)	Grain size (μm)	Condition	References
494	–	–	15	Hot pressing a mixture of Cr/Al/C at 1400 °C with 20 MPa for 1 h in Ar	4
378	–	3.5	20	Hot pressing a mixture of Cr/Al/C at 1400 °C with 20 MPa for 1 h in Ar	7
483	–	5.2	5	Hot pressing an milled mixture of Cr/Al/C at 1400 °C with 30 MPa for 1 h in Ar	12
305	6.2	3.5	35	Hot pressing a mixture of Cr/Al/C at 1450 °C with 30 MPa for 1 h in Ar	Present work
513	4.7	6.4	2	Hot pressing an mechanically activated mixture of Cr/Al/C at 1100 °C with 30 MPa for 1 h in Ar	Present work

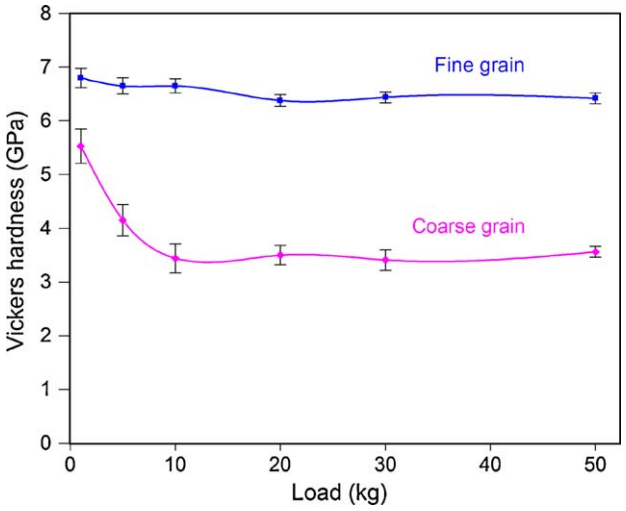

Fig. 7. Vickers hardness versus indentation load for fine-grained and coarse-grained Cr_2AlC.

M–X bonds in the "211" phase series, which contributes to its high elastic modulus, and also to its high strength.

The Vickers hardness of the fine-grained Cr_2AlC is about 6.4 GPa and that of the coarse-grained Cr_2AlC asymptotically approaches about 3.5 GPa, both measured in the load range of 1–50 kg (see Fig. 7). The hardness curves of the fine- and coarse-grained Cr_2AlC show a similar trend in the load range of 1–50 kg (see Fig. 3), namely, the Vickers hardness decreases with increasing load and then asymptotically approaches a constant. Apparently, the effect of grain size on the hardness is predominant. This result is agreed well with that of the fine-gained Ti_2SC (2–4 μm).[44] Also it is reasonable to assume in the present study that the presence of Al_2O_3 may affect the Vickers hardness of the fine-grained samples, because the hardness value of large than 20 GPa[45] for Al_2O_3 is far higher than those for the MAX phase materials.

Analysis of the Vickers indentations as shown in Fig. 8 indicates that the fine-grained Cr_2AlC ceramic is more brittle and thus less damage tolerant than the coarse-grained Cr_2AlC. The Vickers indentation made under a load of 30 kg for the fine-grained Cr_2AlC (see Fig. 8(a)) shows that some of the material is piled-up and some is flaked off around the indentation. Cracks emanated from the indentation corners with a length of about 130 μm. However, similar indentation in the coarse-grained Cr_2AlC (see Fig. 8(b)) does not show any cracks near the corners although significant material pile-up occurred. The damaged zones around the indentations made with a load of 30 kg for the both materials further reveal the damage tolerance mechanism as shown in Fig. 9. For the fine-grained Cr_2AlC, cracks propagate along grain boundaries and the intergranular

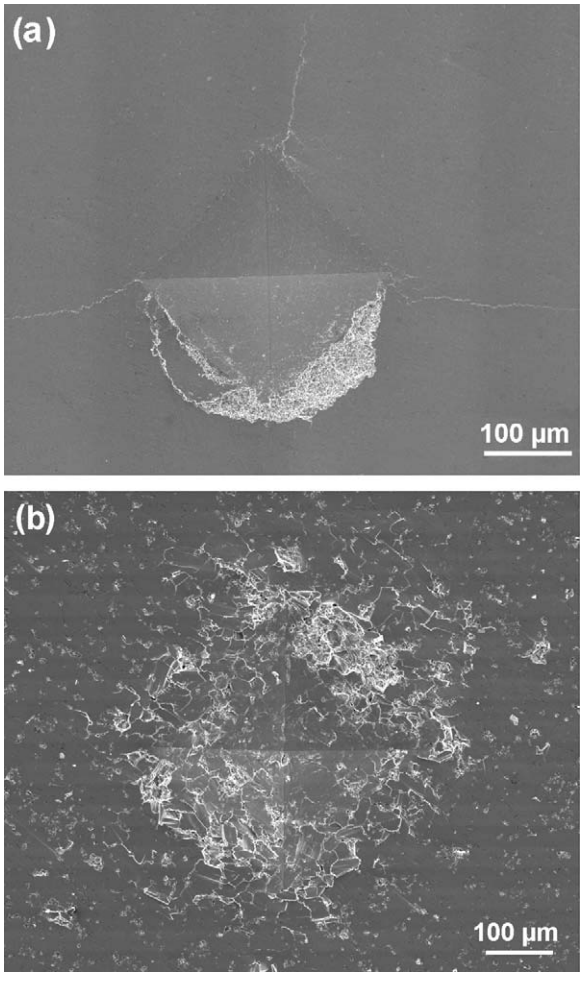

Fig. 8. SEM micrographs of Vickers indentations made under a load of 30 kg for (a) fine-grained Cr_2AlC and (b) coarse-grained Cr_2AlC.

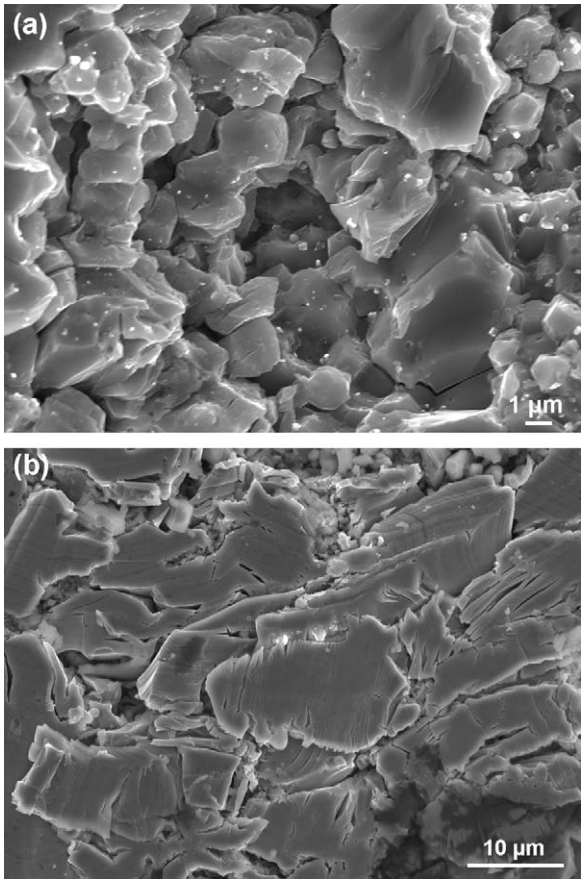

Fig. 9. Enlarged SEM micrographs of the damage zones around indentations taken from (a) and (b) shown in Fig. 8, respectively.

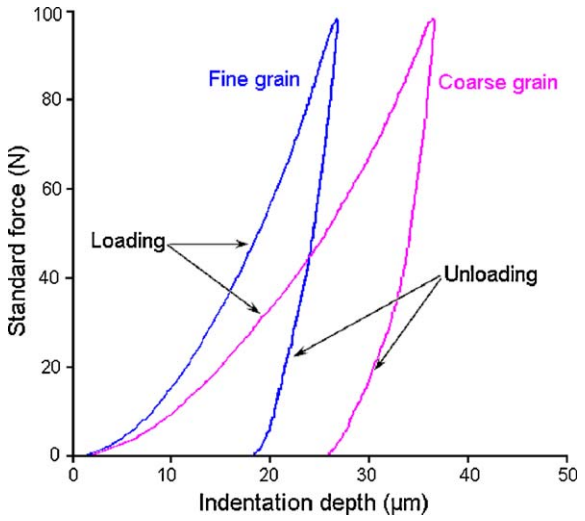

Fig. 10. Loading and unloading curves under 10 kg for fine- and coarse-grained Cr_2AlC.

fracture is dominant. Only a few grains with delamination and buckling of the nano-laminar structure typical for MAX phase ceramics were observed (see Fig. 9(a)). However, for the coarse-grained Cr_2AlC, delamination, kink bands, crack deflection are prevalent (Fig. 9(b)). The multiple energy dissipation mechanism, known for MAX phases materials,[46,47] endows that the coarse-grained Cr_2AlC ceramic with a better damage tolerance.

The difference in plastic response between the fine-grained and the coarse-grained Cr_2AlC ceramics is also evident from the loading and unloading curves (see Fig. 10). The enclosed area after unloading for the fine-grained Cr_2AlC is smaller than that for the coarse-grained Cr_2AlC, indicating that the plastic deformation for the former is smaller than for the latter.

4. Conclusions

A dense Cr_2AlC ceramic with high purity has been successfully synthesized by hot pressing a mechanically alloyed (MA) mixture of Cr, Al and C powders at relatively low temperatures. The enhanced reactivity of MA 2Cr/1.2Al/C powders promotes the formation of Cr_2AlC at a temperature as low as 600 °C.

Due to the high reactivity of the MA powders, the Cr_2AlC ceramic produced at 1100 °C has a high density of 99% and an average grain size of about 2 μm. The flexural strength and Vickers hardness of the dense and fine-grained Cr_2AlC ceramic is 513 MPa and 6.4 GPa, respectively. These properties are much higher than those of the less dense and coarse-grained Cr_2AlC ceramic, viz. 305 MPa and 3.5 GPa, respectively. However, the fracture toughness of the fine-grained Cr_2AlC is 4.7 MPa $m^{1/2}$, which is lower than the 6.2 MPa $m^{1/2}$ for the coarse material. The resistance to plastic deformation of the fine-grained Cr_2AlC is higher than that for coarse-grained Cr_2AlC.

Acknowledgements

This work was supported by the National Natural Science Foundation of China under Grant No. 51072017 and Science Developing Foundation of Beijing Jiaotong University under Grant No. 2007XM034, and the Delft Center of Materials Research Program on Self Healing Materials and Netherlands Innovation Oriented Program on Self Healing Materials under Grant No. IOP-SHM 0871.

References

1. Barsoum MW. The $M_{n+1}AX_n$ phases: a new class of solids; thermodynamically stable nanolaminates. *Prog Solid State Chem* 2000;**28**:201–81.
2. Li SB, Cheng LF, Zhang LT. Oxidation behavior of Ti_3SiC_2 at high temperature in air. *Mater Sci Eng A* 2002;**341**:112–20.
3. Song G, Pei Y, Sloof W, Li SB, De Hosson J, Van de Zwaag S. Oxidation-induced crack healing in Ti_3AlC_2 ceramics. *Scripta Mater* 2008;**58**:13–6.
4. Lin ZJ, Li MS, Wang JY, Zhou YC. High-temperature oxidation and hot corrosion of Cr_2AlC. *Acta Mater* 2007;**55**:6182–91.
5. Tian WB, Wang PL, Kan YM, Zhang GJ. Oxidation behavior of Cr_2AlC ceramics at 1100 and 1250 °C. *J Mater Sci* 2008;**43**:2785–91.
6. Lee DB, Nguyen TD. Cyclic oxidation of Cr_2AlC between 1000 and 1300 °C in air. *J Alloys Compd* 2008;**466**:434–9.
7. Tian W, Wang P, Zhang G, Kan Y, Li Y, Yan D. Synthesis and thermal and electrical properties of bulk Cr_2AlC. *Scripta Mater* 2006;**54**(5):841–6.
8. Hettinger JD, Lofland SE, Finkel P, Meehan T, Palma J, Harrell K, et al. Electrical transport, thermal transport, and elastic properties of M_2AlC (M = Ti, Cr, Nb, and V). *Phys Rev B* 2005;**72**, 115120-1–6.
9. Walter C, Sigumonrong DP, El-Raghy T, Schneider JM. Towards large area deposition of Cr_2AlC on steel. *Thin Solid Films* 2006;**515**:389–93.
10. Manoun B, Gulve RP, Saxena SK, Gupta S, Barsoum MW, Zha CS. Compression behavior of M_2AlC (M = Ti, V, Cr, Nb, and Ta) phases to above 50 GPa. *Phys Rev* 2006;**73**, 024110-1–7.
11. Lin ZJ, Zhou YC, Li MS, Wang JY. In-situ hot pressing/solid–liquid reaction synthesis of bulk Cr_2AlC. *Z Metallkd* 2005;**96**:291–6.
12. Tian W, Wang P, Zhang G, Kan Y, Li Y. Mechanical properties of Cr_2AlC ceramics. *J Am Ceram Soc* 2007;**90**(5):1663–6.
13. Tian W, Sun Z, Du Y, Hashimoto H. Mechanical properties of pulse discharge sintered Cr_2AlC at 25–1000 °C. *Mater Lett* 2009;**63**:670–2.
14. Li SB, Zhai HX, Zhou Y, Zhang ZL. Synthesis of Ti_3SiC_2 powder by mechanically activated sintering of elemental powders. *Mater Sci Eng A* 2005;**407**:315–21.
15. Li SB, Zhai HX, Bei GP, Zhou Y, Zhang ZL. Synthesis of Ti_3AlC_2 by mechanically activated sintering of elemental powders of Ti, Al and C. *Ceram Int* 2007;**33**:169–73.
16. Li SB, Bei GP, Zhai HX, Zhou Y, Li CW. Synthesis of Ti_2SnC at low-temperature using mechanically activated sintering process. *Mater Sci Eng A* 2007;**457**:282–6.
17. Mendelson MI. Average grain size in polycrystalline ceramics. *J Am Ceram Soc* 1969;**52**:443–6.
18. Yang XY, Huang ZW, Wu YK, Ye HQ. HREM observations of the synthesized process of nano-sized SiC by ball milling of Si and C mixed powders. *Mater Sci Eng A* 2001;**300**:278–83.
19. Ghosh B, Dutta H, Pradhan SK. Microstructure characterization of nanocrystalline Ni_3C synthesized by high-energy ball milling. *J Alloys Compd* 2009;**479**:193–200.
20. Mittemeijer EJ, Scardi P, editors. *Diffraction analysis of the microstructure of materials*. Berlin Heidelberg, New York: Springer-Verlag; 2004.
21. Scherrer P. Bestimmung der grösse und der inneren struktur von kolloidteilchen mittels röntgenstralen. *Göttinger Nachrichten Gesell* 1918;**26**:98–100.
22. Suryanarayana C. Mechanical alloying and milling. *Prog Mater Sci* 2001;**46**:1–184.
23. Tian WB, Wang PL, Kan YM, Zhang GJ, Li YX, Yan DS. Phase formation sequence of Cr_2AlC ceramics starting from Cr–Al–C powders. *Mater Sci Eng A* 2007;**443**:229–34.
24. Ma N, Fang X, Liang G, Su J. Influence of mechanical activation on reaction activation energy of Al-Ti-C powder mixture in synthesis process. *Acta Metall Sinica* 2000;**36**:1169–71.

25. Li SB, Zhai HX, Bei GP, Zhou Y, Zhang ZL. Formation of Ti_3AlC_2 by mechanically induced self-propagating reaction in Ti–Al–C system at room temperature. *Mater Sci Technol* 2006;**22**:667–72.
26. Wang ZQ, Liu XF, Zhang JY, Bian XF. Reaction mechanism in the ball-milled Al–Ti–C powders. *J Mater Sci Lett* 2003;**22**:1427–9.
27. Zou Y, Sun ZM, Hashimoto H, Tada S. Low temperature synthesis of single-phase Ti_3AlC_2 through reactive sintering Ti/Al/C powders. *Mater Sci Eng A* 2008;**473**:90–5.
28. Peng C, Wang CA, Song Y, Hong Y. A novel simple method to stably synthesize Ti_3AlC_2 powder with high purity. *Mater Sci Eng A* 2006;**428**:54–8.
29. Okamoto H. Al–Cr. *J Phase Equilib Diffus* 2008;**29**:112–3.
30. Wang XH, Zhou YC. Solid–liquid reaction synthesis and simultaneous densification of polycrystalline Ti_2AlC. *Z Metallkd* 2002;**93**:66–71.
31. Wang P, Mei B, Hong X, Zhou W. Synthesis of Ti_2A1C by hot pressing and its mechanical and electrical properties. *Trans Nonferrous Met Soc China* 2007;**17**:1001–4.
32. Bai Y, He X, Li Y, Zhu C, Zhang S. Rapid synthesis of bulk Ti_2AlC by self-propagating high temperature combustion synthesis with a pseudo-hot isostatic pressing process. *J Mater Res* 2009;**24**:2528–35.
33. Tzenov NV, Barsoum MW. Synthesis and characterization of $Ti_3AlC_{1.8}$. *J Am Ceram Soc* 2000;**83**:825–32.
34. Zhou A, Wang C, Huang Y. Synthesis and mechanical properties of Ti_3AlC_2 by spark plasma sintering. *J Mater Sci* 2003;**38**:3111–5.
35. El-Raghy T, Barsoum MW, Kalidindi SR. Processing and mechanical properties of Ti_3SiC_2: II. Effect of grain size and deformation temperature. *J Am Ceram Soc* 1999;**82**:2855–60.
36. Li SB, Xie JX, Zhao JQ, Zhang LT. Mechanical properties and mechanism of damage tolerance for Ti_3SiC_2. *Mater Lett* 2002;**57**:119–23.
37. Procopio AT, Basoum MW, EL-Raghy T. Characterization of Ti_4AIN_3. *Met Mater Trans A* 2000;**31**:333–7.
38. Ganguly A, Zhen T, Barsoum MW. Synthesis and mechanical properties of Ti_3GeC_2 and $Ti_3(Si_xGe_{1-x})C_2$ ($x = 0.5$, 0.75) solid solutions. *J Alloys Compd* 2004;**376**:287–95.
39. Salama I, El-Raghy T, Barsoum MW. Synthesis and mechanical properties of Nb_2AlC and $(Ti, Nb)_2AlC$. *J Alloys Compd* 2002;**347**:271–8.
40. Zhou Y, Dong H, Wang X, Yan C. Preparation of Ti_2SnC by solid–liquid reaction synthesis and simultaneous densification method. *Mater Res Innovat* 2002;**6**:219–25.
41. Wang J, Zhou Y. Recent progress in theoretical prediction, preparation, and characterization of layered ternary transition-metal carbides. *Annu Rev Mater Res* 2009;**39**, 10.1–10.29.
42. Lin ZJ, Zhou YC, Li MS. Synthesis, microstructure and property of Cr_2AlC. *J Mater Sci Technol* 2007;**23**:721–46.
43. Sun ZM, Ahuja R, Li S, Schneider JM. Structure and bulk modulus of M_2AlC (M = Ti, V and Cr). *Appl Phys Lett* 2003;**83**, 899-891.
44. Amini S, Barsoum MW, El-Raghy T. Synthesis and mechanical properties of fully dense Ti_2SC. *J Am Ceram Soc* 2007;**90**:3953–8.
45. Krell A, Blank P. Grain size dependence of hardness in dense submicrometer alumina. *J Am Ceram Soc* 1995;**78**:1118–20.
46. Li SB, Cheng LF, Zhang LT. Identification of damage tolerance of Ti_3SiC_2 by hardness indentations and single edge notched beam test. *Mater Sci Technol* 2002;**18**:231–3.
47. El-Raghy T, Zavaliangos A, Barsoum MW, Kalidinidi S. Damage mechanisms around hardness indentations in Ti_3SiC_2. *J Am Ceram Soc* 1997;**80**:513–6.